CHAPTER-TWO

PREPARATION OF FERRITES AND CRYSTAL STRUCTURE CHARACTERISATION

CHAPTER - II

2.1 Introduction :

Since 1950, ferrites are extensively used for technological purposes. A wide spectrum of their applications clearly brings out their specific property requirements. As we know that properties of ferrites are structure sensitive, depend on physico-chemical, and physico-thermal history. To meet the requirement of desired application it is a must to have their properties reproduciable. The day by day sophistication in the preparation techniques by different workers, enable us to achieve the target.

As ferrites are the magnetic oxides they do not require special extraction techniques or the techniques involving molten phases. Different co-workers have suggested various methods of preparation for simple, mixed and substitutional ferrites, of known composition and properties in a reproduciable manner. It is found that it is more economical to prepare polycrystalline ferrites by ceramic process with desired microstructure and complex chemical composition than that of single crystal techniques.

In this section a brief survey of methods of preparation of polycrystalline ferrites along with the standard ceramic method and the various factors that influences the microstructure and properties are discussed. The later part of this section is devoted to the actual method used to prepare the ferrite system under study and the crystal structure of ferrite along with techniques used for crystal structure characterisation.

2.2 Methods of Ferrites Preparation :

Almost all techniques of ferrite manufacturing consist of the following four steps.

1) Preparation of intimate mixture with the correct ratio of metal ions required in the final product. 2) Presintering 3) Grinding of presintered material 4) Sintering to obtain final product.

All these four steps followed sequentially irrespective of individuality of preparation techniques.

2.2.1 Oxide method :

In this method high purity oxides are mixed to form intimate mixture with known ratio of metal ions and chemical composition required, mixing is always done wet milling in rubber lined pot using stainless steel balls. Some times rotary ball mill method is also used to cut milling time. After milling the material, it is dried and pressed into required shape, presintered and final sintered to obtain desired product. The drawback of this method is that the possibility of mixing steel in the ball milling process and is supported by Blackman's[1] studies on $Mg_{0.9}Mn_{0.1}Fe_{1.6}O_{3.4}$ system.

2.2.2 Decomposition :

In this method carbonates, nitrates, and oxlates are mixed in the required propertions and preheated in air to produce oxides by thermal decomposition. Remaining part of this method is same to that of the oxide method. The success of this method again lies in the formation of homogenous mixture. The added advantage of this method is that oxides thus produced would readily undergo solid state reaction[2].

2.2.3 Hydroxide precipitation :

To avoid lengthy milling time and laborous work, attempts have been made to precipitate hydroxides from a given solutions, so that the precipitation contains metal ions in requisite propertions. The success of this method lies in the simultanity achieved in precipitation, for this one requires the complete understanding of the process and of the solubility product. The completness of precipitation can be ensured by the pH value calculated from solubility product Economas[3] established this method which is further used by Wolf and Rodrigue[4] to prepare yattrium iron garnet. Later on by hydroxide coprecipitation method, Sato[5] has prepared ultrafine spinel ferrite.

2.2.4 Oxlate precipitation :

In this method metallic oxlates are precipitated using amonium oxlate, which does not leave any residue after ignition. Most of the metal oxlates are having similar crystal structure, therefore precipitation leads to produce the final product with desired cation ratio. The merit of this in mixing of the materials with correct ion ratio on molecular scale[3].

2.2.5 Presintering, pressing and sintering :

Presintering : The purpose of presintering according to Swallow and Jorden[6] is to decompose carbonates and higher oxides so as to avoid evolution of gas during final sintering. It also helps in homogenizing and reducing compositional variation of raw materials. Presintering keeps in control the shrinkage that occurs in final sintering. In presintering partial formation of the final product occurs. The extent of the solid state reaction on presintering depends upon the reactivity of the chemical constituents and temperature used[6].

Pressing or extrusion : The dry powder is mixed with organic binder, 1% polyvenyl alcohol or 1% ammonium alginate and pressed to desired shapes by apply ing pressuresd that ranges from 1 to several tons/inch^2.

Sintering : This is the final and critical step in which the presintered and pressed material is heated at a temperature of 1000°C for about 48 hours. In this process ferrite is formed by interdiffusion between the adjacent particles. They sick or sinter together because at this temperature ferrite has a good plasticity.

The correct control of partial pressures of oxygen in the furnace during the entire cycle is maintained to avoid reduction of sample. To obtain the desired microstructure the following factors are to be kept in control.

2.2.6 Atmosphere :

In order to achieve the desired stoichometry and correct valance state that remains unaffected by further oxidation or reductions requires correct control of partial pressure of oxygen in furnace and temperature. The problem oftenly comes with metals like Fe, Mn, Cu and Co which changes their valence states rapidly[7]. Effect of furnace atmosphere on magnetite (Fe_3O_4) was extensively studied by Darkeen's and Gurry[8]; Smiltens[9] and by Economs[3]. It is found that oxygen deficiency causes iron and some other to exist in more than one valence states. Excess of oxygen on the other hand results in cation vacancies. Excess Fe^{2+} and simultaneous presence of Fe^{3+} gives the electrical conduction $Fe^{2+} + e = Fe^{3+}$ with low activation energy and hence decrease of resistivity. The effect of furnace atmosphere on ferrites is also reported by Paladino[10], Woodhouse and White[11].

2.2.7 Grain size control :

As temperature increases the average grain size increases due to decrease in grain boundry energy. The grain boundry during grain growth moves towards the centre of curvature. The grains having more than six surfaces grows at the expense of their small neighbourers. The grain growth takes place according to the expression

$$D - D_o = Kt^n \quad \ldots \quad (2.1)$$

where D_o is original particle size, K be the temperature dependent factor and t a time.

If the average grain size reaches a critical value then discontinuous grain growth takes place. In discontinuous grain growth, grain size increases over all matrix size and may form duplex structure. Zener[12] has given an empirical relation for discontinuous grain growth as

$$D_{cr} = \frac{di}{fi} \quad \ldots \quad (2.2)$$

where di is the diameter of inclusion and fi is the volume fraction of inclusion.

Presence of impurity, chemical inhomogeneity and variation in density influences the discontinuous grain growth. To keep the grain size in control it is to start with extremely high purity oxides, with small particle size. Use of hot pressing technique helps to control the grain size.

2.2.8 Porosity :

It is the characteristics of sintered ceramics in which powder compaction is used. Physical origin of porosity lies in the difference of X-ray and physical density of the material given by percentage porosity. The low porosity and fine grains is often required in ferrites, but it is extremely difficult in

ceramic process. Lower sintering rates gives high porosity, and enhances the grain growth. Therefore, to obtain low porosity sintering rate is accelerated. In ceramic method, double sintering process helps in decreasing the porosity and in increasing the physical density. The porosity and grain size can be controlled by using hydroxide co-precipitation and hot pressing techniques. The studies on sintering process by Reijnen[13] have clearly shown that effect low sintering rate on microstructure development.

Repetitions of heating cycles all the time does not help in increasing the densification because the pores at grain boundaries only can be removed by heating, while entrapped pores during discontinuous grain growth requires a large amount of energy and hence at ordinary conditions they remain as such giving us all the time porosity.

2.2.9 Effect of sintering temperature:

Average grain size and permeability increases with increase of temperature, but the effect of later is less than first. The temperature also decides grain distribution and orientation of cystallites. Ram Prasad and V.K.Murthy[14] have reported the increase of density with increase of sintering temperature or time. The sintering temperature greater than critical temperature will have no densification effects, but may deteriorate the performance of permeability at higher frequencies.

2.2.10 Hot pressing :

The technological requirement of small grain size, low porosity and high density at low sintering temperature can be achieved by the use of hot pressing. A continuous hot pressing method was developed by Gruintjes and Oudemans[15], which was later used by de Lau[16]. The success of this method lies

Flowchart of the stages in the ferrite preparation.

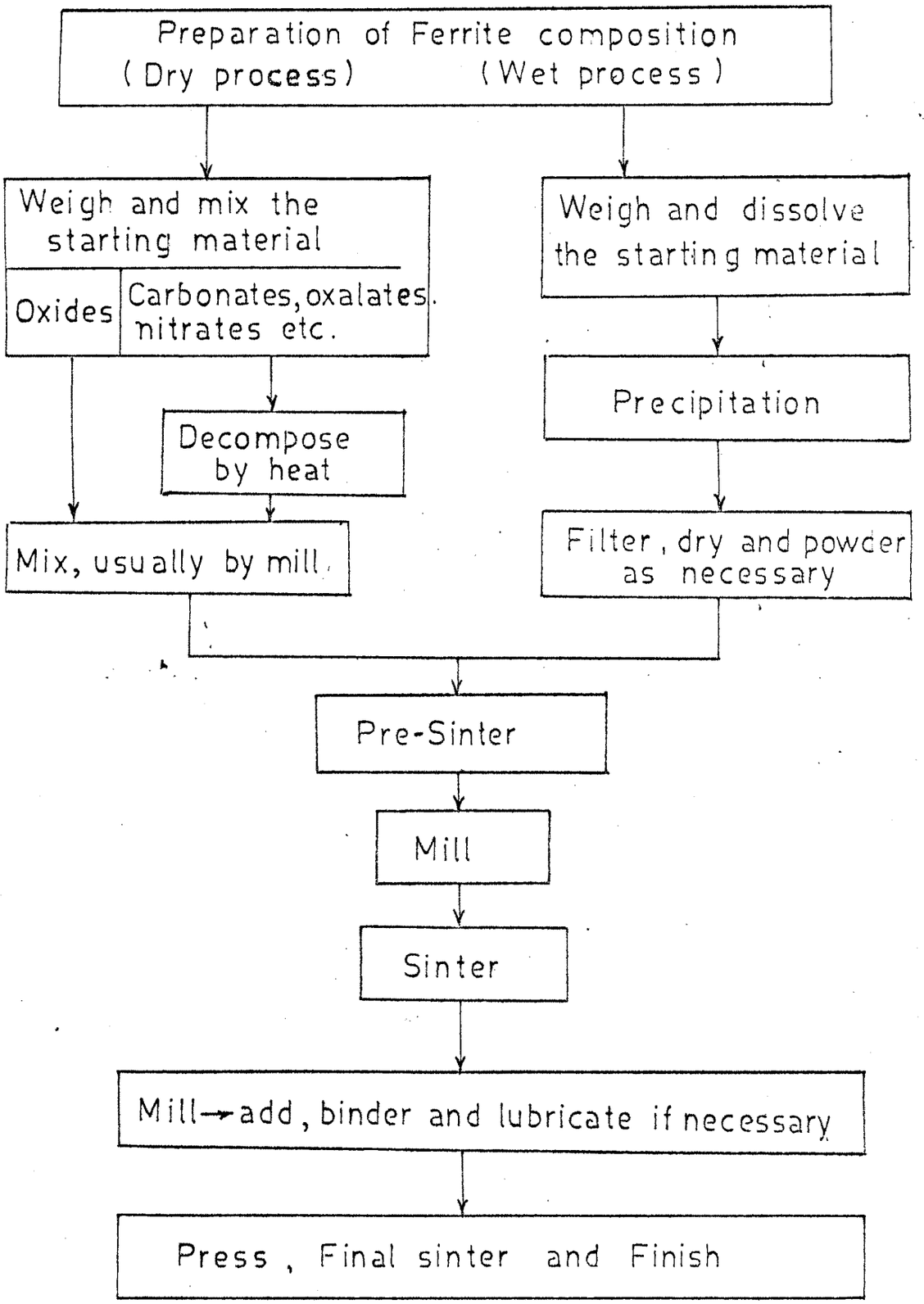

in its principle, in which a simultaneous application of temperature and pressure[7]. High density and low porosity with original particle size is due to accelerated sintering rate. The hot pressing pressure leads to high degree of compaction and enhances grain to grain contact. The rising hot pressing pressure may vary the composition, concentration of Fe^{2+} ions in ferrite and the degree of inversion.

2.3 Flow Chart : (As shown)

2.4 Preparation of Ferrite under Investigation :

Ferrites can be prepared by several methods discussed so far; out of these ceramic method is rather simple and is commercial, because high purity oxides are readily available. We have therefore, used ceramic method of preparation for the system under investigation.

General formula : The general chemical formula of the ferrite system under investigation is $Zn_xMg_{1-x}Fe_2O_4$ doped with 0.01 mol. wt. %and without doping. where x = 0, 0.2, 0.4, 0.6, 0.8, 1.0.

Raw materials :

1) A.R.grade Fe_2O_3 from Riedel - German made 99.5% pure.

2) A.R. grade ZnO. 3) A.R. grade MgO.

4) A.R.grade ZrO_2, Indian Rare earth limited, Govt. of India, Mineral division.

Weighing : The required raw materials weighed on a single pan microbalance of least count 10^{-5} gm, and were mixed according to their molecular weight proportions and doped with 0.01 % ZrO_2.

Milling : The oxides mixed in the molecular weight proportions are taken in agate mortor and is mechanically blended in A.R.grade acetone, for two hours

so as to form the intimate mixture. Then the mixture is allowed to dry in air and carefully transferred to clean and dry platinum crucible. The same procedure is repeated for all samples.

Presintering : The platinum crucibles are kept in glow bar furnace and the furnace is heated at the rate of 80°C per hour, upto 800°C for 24 hours. The temperature of furnace was controlled by dimerstat, and care is taken to keep the required partial pressure of oxygen in the furnace throughout the entire heating period. The furnace was then cooled at the rate of 80°C per hour down to room temperature. To measure the furnace temperature calibrated Chromel-alumel thermocouple was used.

Grinding : The crucibles are taken slowly out of the furnace, and samples were transferred to clean agate mortor, and grinded to form the fine powder. The grinding in A.R.grade acetone was carried out for three hours for each sample to obtain the original particle size. They are sieved and reground to obtain the uniform particle size.

Sintering : The samples were transferred to clean and dry crucible washed with chromic acid. Crucibles were kept in glow bar furnace and the furnace was heated at the rate of 80°C per hour so as to obtain the 1000°C temperature in about 12 hours. The furnace was kept at 1000°C constant temperature for forty eight hours. Furnace temperature and atmosphere was carefully controlled so as to obtain the desired microstructure. The furnace was then cooled at the same rate of 80° per hour down to room temperature by reducing the current.

Pellet formation : The sintered samples were ground in acetone base and were sieved to obtain uniform particle size. Then with help of punch die of 1 cm diameter and pressure of 10 tonnes per square inch, pellets were formed. The solution of 5% polyvenyl acetate was used as an organic binder.

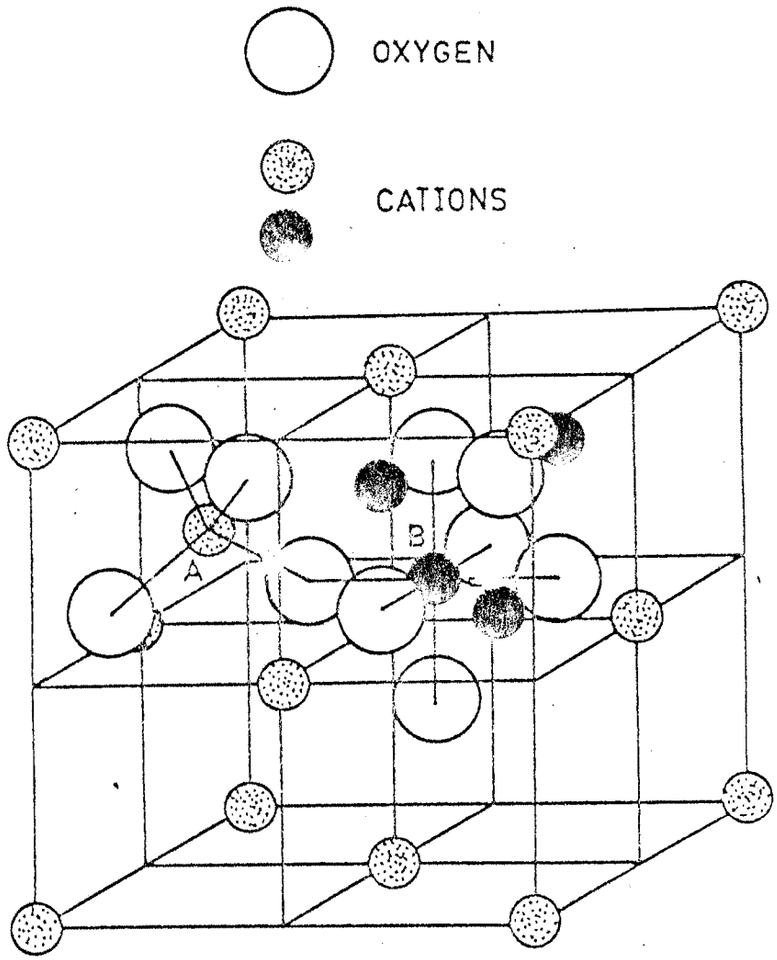

FIG.2·1: THE SPINEL STRUCTURE.

Final sintering : The pellets so formed were kept on thin platinum foils, and the platinum foils were kept in glow bar furnace. The furnace was heated at the rate of 80°C per hour upto 1000°C in about 12 hours. The furnace was kept at constant temperature of 1000°C for 12 hours. The due care is taken to control the furnace temperature and atmosphere so as to avoid the reduction of samples. The furnace was then cooled at the rate of 80°C per hour down to room temperature.

Polishing : The pellets were polished smooth with fine metal polish paper, so that opposite faces becomes exactly parallel to each other. The thickness of the pellets were maintained almost equal.

2.5 Crystal Structure of Ferrites :

Ferrites are having spinel structure. The word spinel is from mineral spinel $MgAl_2O_4$ (see fig.2.1). All spinel ferrites have face centred cubic crystal structure, that belongs to a space group O^7_h-fd 3m. The general chemical formula for such a ferrites is given by $M^{2+}Fe^{3+}O^{2-}$ or $MOFe_2O_3$; where M is any divalent metal ion usually the member of first or second transition series such as Mn^{2+}, Fe^{2+}, Co^{2+}, Ni^{2+}, Zn^{2+}, Cd^{2+} etc. There are eight molecules of MFe_2O_4 per unit cell. The anions (oxygen) which are having large radius forms ideally a face centered lattice. The cations having small size occupies the interstitial positions. Totally there are 96 interstitial positions, which are divided into two lattice sites, namely the tetrahedral (A), and Octahedral (B) site. Out of these 96 interstitial positions, 64 are tetrahedral (A) and 32 are octahedral (B) sites. In a unit cell, out of 64 A sites only 8 are occupied by metal ions, which are surrounded by four oxygen ions. Fig.(2.2), while out of 32 B sites only 16 are occupied by metal ions surrounded by six oxygen ions, see fig.(2.3). When the packing parameter u=3/8, the packing is

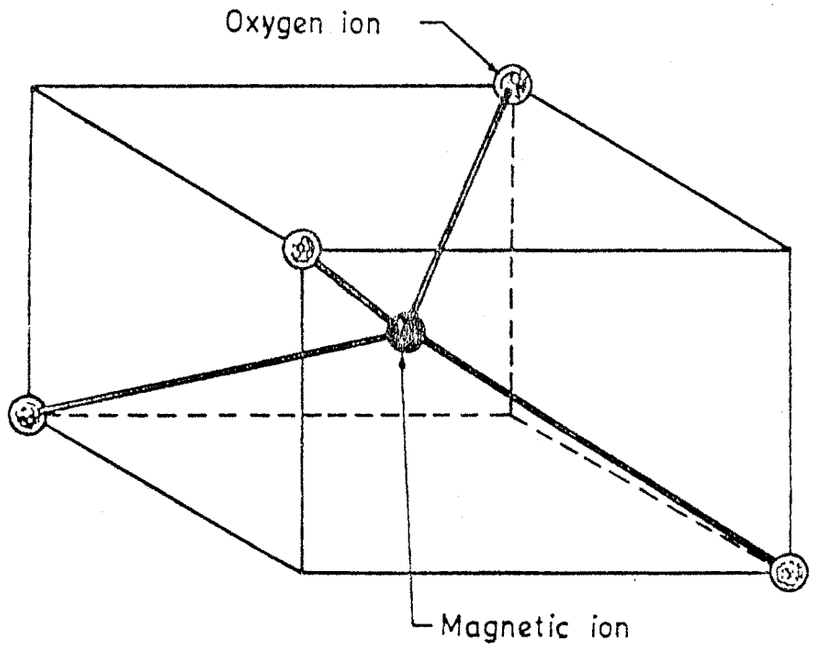

Fig. 2.2 : THE MAGNETIC ION OCCUPIES A "TETRAHEDRAL LATTICE SITE" WHERE IT IS SURROUNDED BY FOUR NEAR-NEIGHBOUR OXYGEN IONS.

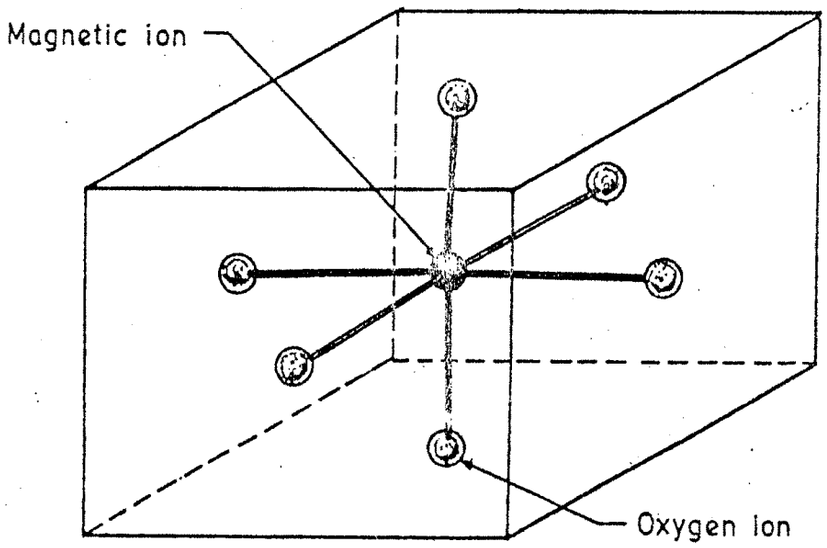

Fig. 2.3 : THE MAGNETIC ION IS SAID TO OCCUPY AN "OCTAHEDRAL LATTICE SITE" WHERE IT IS SURROUNDED BY SIX NEAR-NEIGHBOUR OXYGEN IONS.

considered to be the perfect[18]. The distribution of 24 metal ions into A and B sites is determined by site preference energies of different cations.

According to Goodenough and Loeb[19], the site preference energies have a considerable contribution in cation distribution. Classification of spinel ferrites is done on the basis of the cation distribution into normal spinel, inverse spinel and random spinel. When a trivalent metal ion in single ferrites is substituted by an equivalent another metal ion, the substitutional ferrites are formed[22].

2.5.1 Normal spinel ferrites :

In normal spinel eight metal ions (M^{2+}) occupies A sites and Fe^{3+} ions occupies B sites given by the catioin distribution of the type

$$(M^{2+})\ [\ Fe^{3+},\ Fe^{3+}\ ]^{B}\ O_4^{2-} \qquad \ldots \qquad (2.3)$$

$ZnFe_2O_4$ and $CdFe_2O_4$ are the normal spinels. The cation distribution of $ZnFe_2O_4$ is given as

$$(Zn^{2+})^{A}\ [\ Fe^{3+},\ Fe^{3+}]^{B}O_4^{2-} \qquad \ldots \qquad (2.4)$$

It is experimentally observed that normal spinels are non-magnetic in nature.

2.5.2 Inverse spinel ferrite :

In inverse spinel, the eight metal ions (M^{2+}) occupies B sites, and eight (Fe^{3+}) occupies A sites, while remaining $8Fe^{3+}$ occupies B sites. The cation distribution of the inverse spinel can be given as

$$(Fe^{3+})^{A}\ [\ M^{2+}Fe^{3+}]^{B}O_4^{2-} \qquad \ldots \qquad (2.5)$$

The magnesium ferrite ($MgFe_2O_4$) and copper ferrite ($CuFe_2O_4$) are inverse spinels showing cation distribution as above. The cation distribution of the $MgFe_2O_4$ ferrite is

$$(Fe^{3+})^{A}\ [\ Mg^{2+}Fe^{3+}\ ]^{B}O_4^{2-} \quad \ldots \quad (2.6)$$

It is observed that inverse spinels are magnetic in nature.

2.5.3 Random spinel ferrites :

The normal and inverse spinel ferrites are the extreme cases of spinel ferrites. X-ray and neutron diffraction studies have disclosed some intermediate structure in which the 24 metal ions are randomly distributed into A and B sites, called as random spinel ferrites. In such a ferrites distribution of metal ions into A and B sites is influenced by compositional variation, physico-chemical and thermal conditions of preparation. The single ferrites $MnFe_2O_4$ and $CoFe_2O_4$ are the random spinels with 20% and 74% inversion respectively. The studies on $CoFe_2O_4$ by Vaingankar[20] et al. have reported that $CoFe_2O_4$ is 74% inverse.

The cation distribution of partially inverse or random spinel ferrites is given by

$$(M\ \ Fe_{(1-\ )})^{A}\ [M_{1-}\ Fe_{(1+\ )}]^{B}\ O_4^{--} \quad \ldots \quad (2.7)$$

where is known as coefficient of inversion or normalacy. The cation distribution of $MnFe_2O_4$ is given by

$$(Mn^{2+}_{0.8}Fe^{3+}_{0.2})^{A}\ [Mn^{2+}_{0.2}Fe^{3+}_{1.8}]O_4^{--} \quad \ldots \quad (2.8)$$

In ferrites every oxygen ion is surrounded by three B cations, and one A cation. The angles[21] are given as A - O - B = 125°9', A - O - A = 79°58', B - O - B = 90°, see fig. (2.4). The interaction is expected to be strong if M-O-M distance is small and the angle M-O-M equal to 180°.[22] Therefore, it can be concluded that A-A and B-B interactions are weak and only A-B interaction is strong. In general for all ferro spinels all interactions are negative.

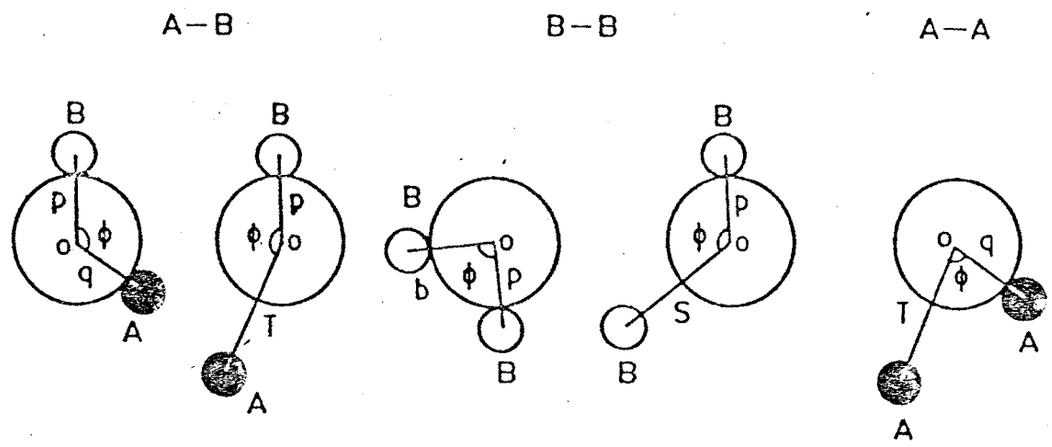

O = 125°9′ 154°34′ 90° 125°9′ 79°38′

Fig.2·4: ANGLE BETWEEN A-A, B-B & A-B CATIONS IN A SPINEL STRUCTURE.

2.5.4 Substitutional ferrites :

In substitutional ferrites (Fe^{3+}) ions are replaced by Al^{3+}, Ga^{3+} or Cr^{3+}.[22] The net magnetisation in such a ferrites depends on the site preference of substituent. In a aluminium substituted ferrites the net magnetisation decreases because Al^{3+} prefers octahedral (B) site, while Ga^{3+} substituted ferrites magnetisation increases because Ga^{3+} preferably occupies tetrahedral (A) site. For example if in Nickel ferrite ($NiFe_2O_4$) when a part of trivalent iron ion replaced by Al^{3+} then the resulting compound takes the form $NI\ Fe_{2-y}Al_yO_4$ called nickel ferrite aluminate.

2.6 Structural Co-ordinates of Cubic Spinels :

The structural co-ordinates of the tetrahedral and octahedral cations and oxygen ions for cubic system is given by Wyckoff[23]. The ionic positions are as under

Anion 32b	(u, u, u); (u, u, u); (u, u, u); (u, u, u); (1/4-u, 1/4-u, 1/4-u), (1/4-u, u+1/4, u+1/4); (u+1/4, 1/4-u, u+1/4); (u+1/4, u+1/4; 1/4-u);
Cation 16c	(5/8, 5/8, 5/8); (5/8, 7/8, 7/8); (7/8, 5/8, 7/8); (7/8, 7/8, 5/8);
cation 8f	(0, 0, 0); (1/4, 1/4, 1/4);

With the translations, for a face centered lattice,

(0, 0, 0); (0, 1/2, 1/2); (1/2, 0, 1/2); (1/2, 1/2, 0).

2.7 Parameters Involved in Spinel Ferrites :

There are number of different metallic ions in spinel lattice. They are accommodated in spinel lattice in such a way that they must be small enough to keep the oxygen ions near to each other so as to form the stable structure. The radius of oxygen ion is 1.32A°. The radai of most metallic ion occuring in spinel lie between 0.5 an 1A°. The charge of the ions may be anything between 1 and 6[24]. The lattice parameter[9] for most of the cubic ferrites ranges from 8.3A° upto 8.5 A°[25]. The oxygen ion positions are defined by a crystallographic parameter u, which generally lies between 0.378 and 0.400[26]. The distance between the tetrahedral site (0,0,0) and the oxygen site (3/8,3/8, 3/8) is U_{ideal} = 3/8. For divalent cations, U_{obs} is always larger than U_{ideal} due to the stronger expansion of the tetrahedral interstices at the expense of the octahedral sites. The grain size of commercial ferrites ranges from about 5 μ to 40 μ.

The interatomic spacing or bond distance or metal to oxygen ion distance from tetrahedral A-site and octahedral B-site of the spinel lattice (cubic or tetragonal) can be calculated by using the following relations.

For tetragonal A-site, the interatomic distance is given by

$$A - O = a\sqrt{3}\,(1/8 + \delta) \qquad \ldots \qquad (2.9)$$

For octahedral B-site, the interatomic distance is given by

$$B - O = a\sqrt{\frac{1}{16} - \frac{\delta}{2} + 3\delta^2} \qquad \ldots \qquad (2.10)$$

where 'a' is lattice parameter. The value of 'δ' depends on oxygen 'u' parameter and is given by

$$= u - 0.375 \qquad \ldots \qquad (2.11)$$

is the deviation from the ideal 'u' value.

The radii of the ions on tetrahedral A-sites and octahedral B site are given by [27]

$$r_A = (U - 1/4)\, a\sqrt{3} - r(O_4^{2-}) \qquad (2.12)$$

$$r_B = (5/8 - U)\, a - r(O_4^{2-}) \qquad (2.13)$$

A simple empirical relation between the lattice parameter 'a' and the ionic radii of the cations in the spinel is given by Mikheev[28] as

$$a = 5.778 + 0.95\ A + 2.79\ B \qquad (2.14)$$

The percentage porosity (P) of a ferrite material is given by the expression

$$P = \left(\frac{\rho x - \rho a}{\rho x}\right) \times 100 \qquad (2.15)$$

where, ρa is the apparent density and ρx is the X-ray density of the ferrite material.

The X-ray density in turn is given by the expression

$$x = \frac{8M}{Na^3} \qquad (2.16)$$

where, M is the molecular weight, a is the lattice parameter of the ferrite material and N is the Avagadro's number.

2.8 Diffraction Study :

The X-ray, Neutron and Electron diffraction methods are often used for the determination of crystal structure of solids. These tools are well established and have played a prominent role in the analysis of geometrical shapes of solids.

2.8 a X ray diffraction :

It is a very powerful tool for the analysis of crystal constituents, was used for the first time in 1912 by German physicist, Max von Laue. During the

same year, W.H.Bragg and W.L.Bragg[28] the two English physicist have made analysis of Laue experiment. The most striking contribution of their analysis is the famous formula called Bragg's law and is given by

$$n\lambda = 2\ d\ \sin\theta \qquad (2.17)$$

where 'λ' is wavelength of X-rays and 'd' be the interplaner distance.

X ray diffraction methods : From the observation of Bragg's diffraction condition (2.17) it can be revealed that the law can be put in experiment by two ways, either by varing λ or θ .

When X-ray are incident on the crystal lattice, they get diffracted, when Bragg's condition is satisfied. The diffraction condition can be satisfied by either varying λ or θ . The way in which and are varied discloses the three different methods as Laue method, Rotating crystal method and Powder method.

We can have in short the brief survey of all these methods by tabular form given below

	Method	λ	θ
1)	Laue method	Variable	Fixed
2)	Rotating crystal method	Fixed	Variable
3)	Powder method	Fixed	Variable

The most advantageous method among these three, is the powder method which does not require single crystal specimens. It also determines the lattice parameter to a great accuracy and can identify phases.

Due to the versatality of X-ray diffractions, their applicability is not only restricted to determine crystal structure but also in studies of many diverse phenomenas such as chemical analysis and stress measurements.

2 8.b Electron diffraction :

The investigations of structure of thin foils and films cannot be done by X rays because of their high penetrating power. The electrons with small penetrating power are then useful. The principle involved is same to X-rays but the only difference is that, electron diffraction is restricted to certain depth upto 1000 A° or less. Electron diffraction is advantageous than that of X ray because of efficiency, while both are restricted to higher values, giving weak scattering intensities.

2.8.c Neutron diffraction :

The X-ray and electron diffraction differs from neutron diffraction in a sense that scattering factor of later is independent of scattering angle and atomic number 'z'. It means that some lighter nuclei may scatter neutrons effectively than that of the heavy nucleii. The use of X-rays and electron diffraction is essentially restricted to higher nucleii because of scattering proportionality with atomic number 'z' and will not see light nucleii due to their small scattering factor. Hence neutron diffraction will be very useful in studies of light nucleii.

2.9 X ray Diffraction Study :

For the characterisation of crystal structure and confirmation of ferrite formation of the ferrite system under investigation, we have used the X-ray diffraction technique. The foregoing discussions include X-ray diffractometer

and the study of X-ray diffractograms from which the crystallographic data of the ferrite system $Zn_xMg_{1-x}Fe_2O_4$ before and after doped with 0.01 mole wt.% ZrO_2 were obtained.

2.9.1 The diffractometer :

The diffractometer uses a monochromatic radiation, and can be put to investigate single or polycrystalline specimens. The principle of operation of diffractometer and its essential components are as shown in figure (2.5).

A powder specimen 'c' in the form of a flat plate is placed on table 'H' capable of rotating about an axis 'O'. The diverging beam of X-ray from the sdource 's' after passing through filters, becomes monochromatic eliminating '$K\alpha$' radiation, and are colimiated by a slit 'A' to make incident on the specimen 'c.' The '$K\alpha$' radiations are diffracted by the specimen to form a convergent beam, that passes slit 'B' and focusses at 'F' and then enters the counter G. The carriage 'E' which is free to rotate about an axis 'O' holding the receiving slits moved through an angle of '2θ' of which measurements can be made on scale 'k'. The mechanical coupling between 'E' and 'H' is such that rotation of carriage through '2θ' for the specimen. Coupling also ensures that the angles of incidence and reflection from the specimen are equal and equal to half of total angle of diffraction.

In order to obtain continuous diffraction patterns, counter is driven at a constant angular speed with increasing values of '2θ' until the desired range is scanned. At the same time the recorder moves through angle 2θ proportional to length.

In the present investigation we have used Philips diffractometer (type P.W.1051) with filtered $CuK\alpha$ radiation (λ = 1.542 A°) from X-ray tube operating at 30 kV and 20 mA. From Indian Institute of Technology, Bombay, the

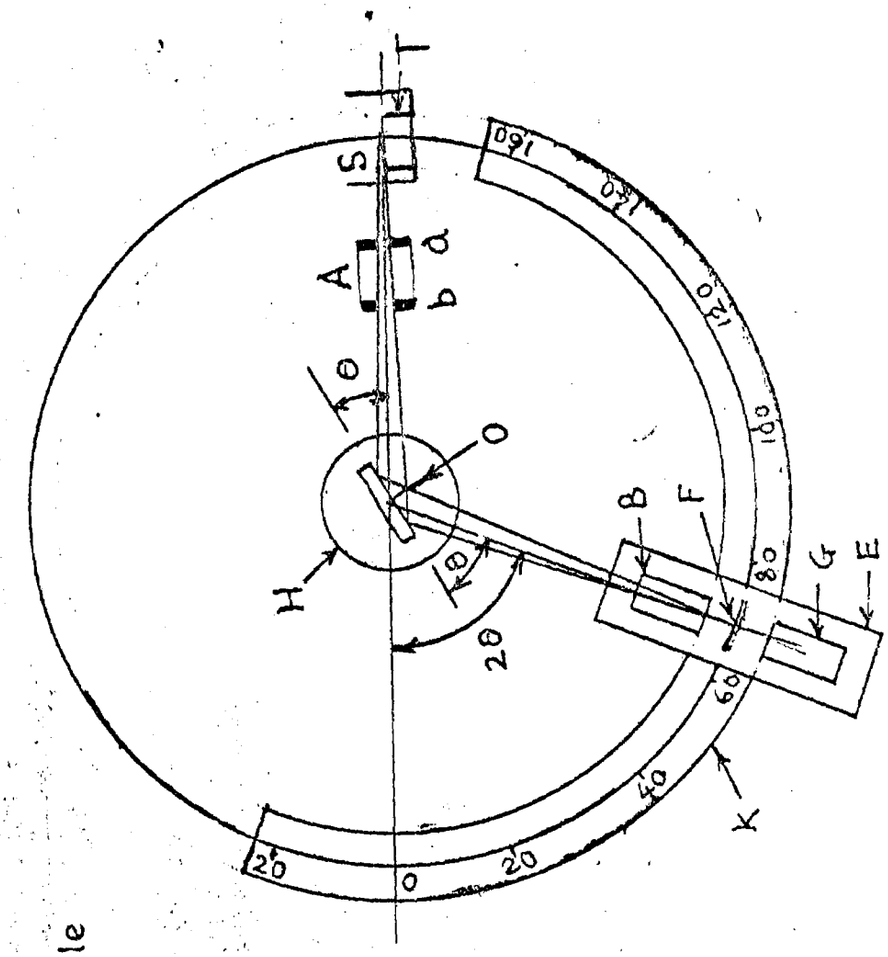

Fig. 2·5:X-ray diffractometer schematic

K–Circular scale
G–Counter
E–Carriage
B,F–Slit
C–Specimen

powder samples of the ferrite system $Zn_xMg_{1-x}Fe_2O_4$ before and after doping with 0.01 mol. wt. % were used for diffraction studies.

Preparation of Samples :

A microslide of size 2.5 cm x 2.5 cm was taken with thin coating of Melrock 211 compound (silicon) was applied on an area of 3.00 cm by 2.5 cm. Fine powder of ferrite sample under investigation was spread uniformally over a coated portion. Sample prepared in this way was kept on holder c.

All the samples were scanned for '2θ' values between 15° and 80° as the lattice is f.c.c. with 'a' values ranging from 8A° to 9A°, and the first reflection at about $2\theta = 18°$.

Indexing the diffractograms :

For a cubic lattice the interplaner distance d_{hkl}, the lattice parameter a' and Millar indices h,k,l are related by

$$d_{hkl} = \frac{a}{h^2+k^2+l^2} \qquad (2.18)$$

comparing it with Bragg's law we get

$$\sin^2 \theta_{hkl} = \frac{\lambda^2}{4a^2} (h^2+k^2+l^2) \qquad (2.19)$$

As hkl are integers, the sum of their squares will also be an integers. Value of $\lambda^2/ 4a^2$ was found from higher '2θ' values, from which lattice parameter 'a' can be determined. The peaks were indexed for which observed and calculated 'd' values are in good agreement.

2 10 Results and Discussion :

The X-ray diffraction technique is employed for the characterisation of crystal structure of the systems under investigations. The X-ray diffractograms are obtained for slow cooled samples of $Zn_xMg_{1-x}Fe_2O_4$ ferrite system before and after doping with 0.01 mol. wt. % ZrO_2 and the same are presented in figures 2.6 to 2.17, The 'd' values are calculated from the formulae given by 2.18 and 2.19. By comparing observed and calculated 'd' values Miller indices (h k l) of the reflecting planes are indexed. The comparative statement of observed and calculated 'd' values, along with the planes at respective '2θ' values are given in table 2.1 to 2.12.

From the diffractograms, it can be seen that, all the samples show well defined diffraction peaks, with no ambigious reflections, which can be immediately noted. The strong reflection peak in all samples is from plane (311). The observed 'd' values are found to be in good agreement with calculated 'd' values. The reflections observed in respect of our system before and after doping for all the samples correspond to the allowed reflections for spinel structure[29], which confirms the preparation and formation of single phase, mixed $Zn_xMg_{1-x}Fe_2O_4$ and $Zn_xMg_{1-x}Fe_2O_4$ ferrite system doped with 0.01 mol. wt. % ZrO_2.

The lattice parameter 'a' is calculated for all samples of the system under investigation before and after doping with 0.01 mol. wt.% ZrO_2 by using the formula 2.19. The calculated values of lattice parameter 'a' shows variation in the range of 8.33 A° to 8.43 A° which is in the range of f.c.c. spinels and it also shows good agreement with the reported values for the same system[30]. The comparative statement of the data, of lattice parameter 'a' is given in table 2.13 and 2.14 before and after doping respectively. From the

FIG : 2.6. $MgFe_2O_4$(LO)

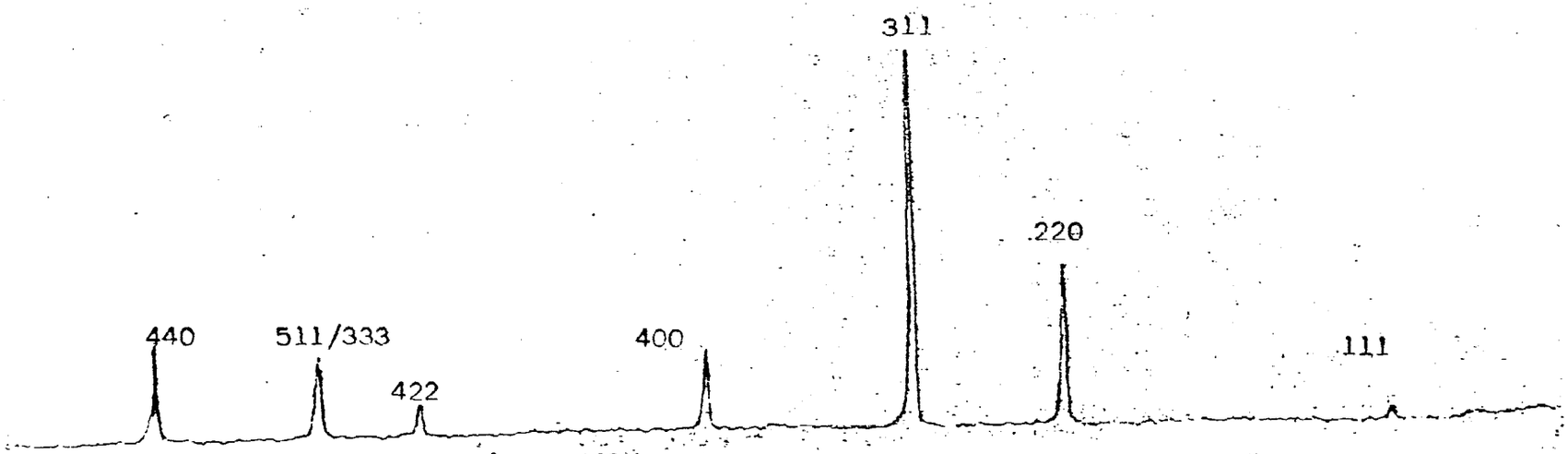

FIG : 2.7. $Zn_{0.2}Mg_{0.8}Fe_2O_4$ (L2)

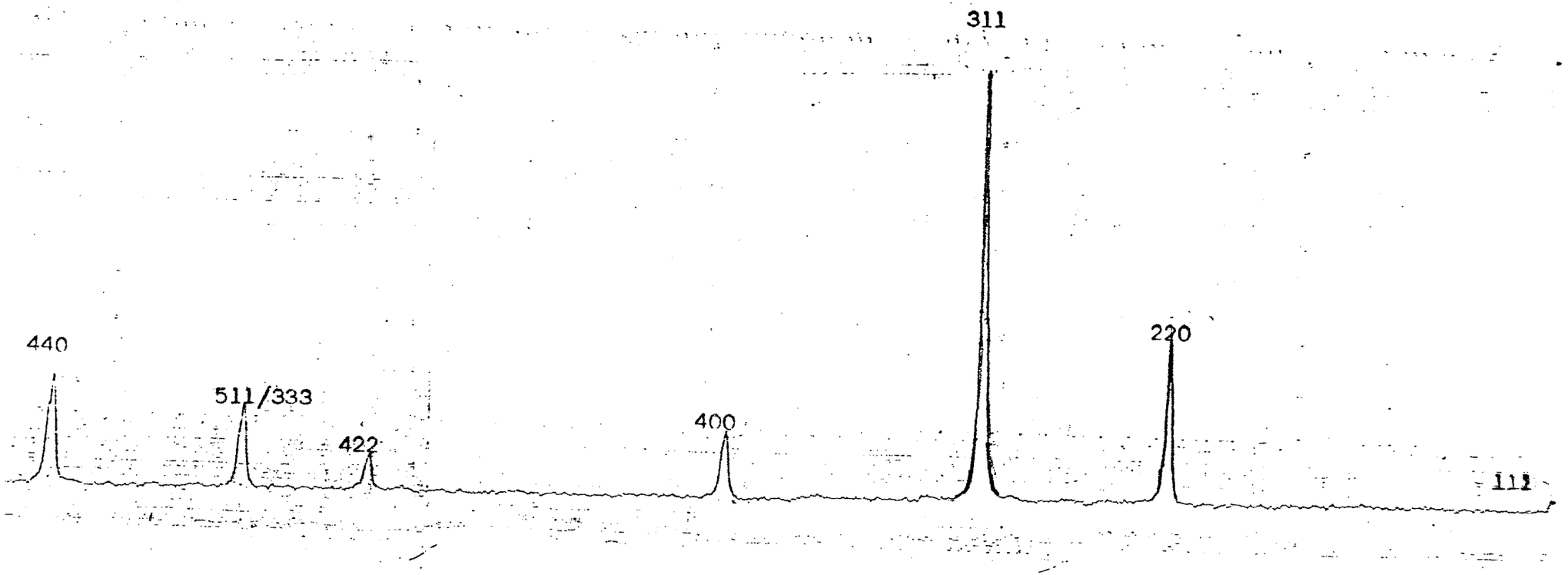

FIG : 2.8. $Zn_{0.4}Mg_{0.6}Fe_2O_4$ (L4)

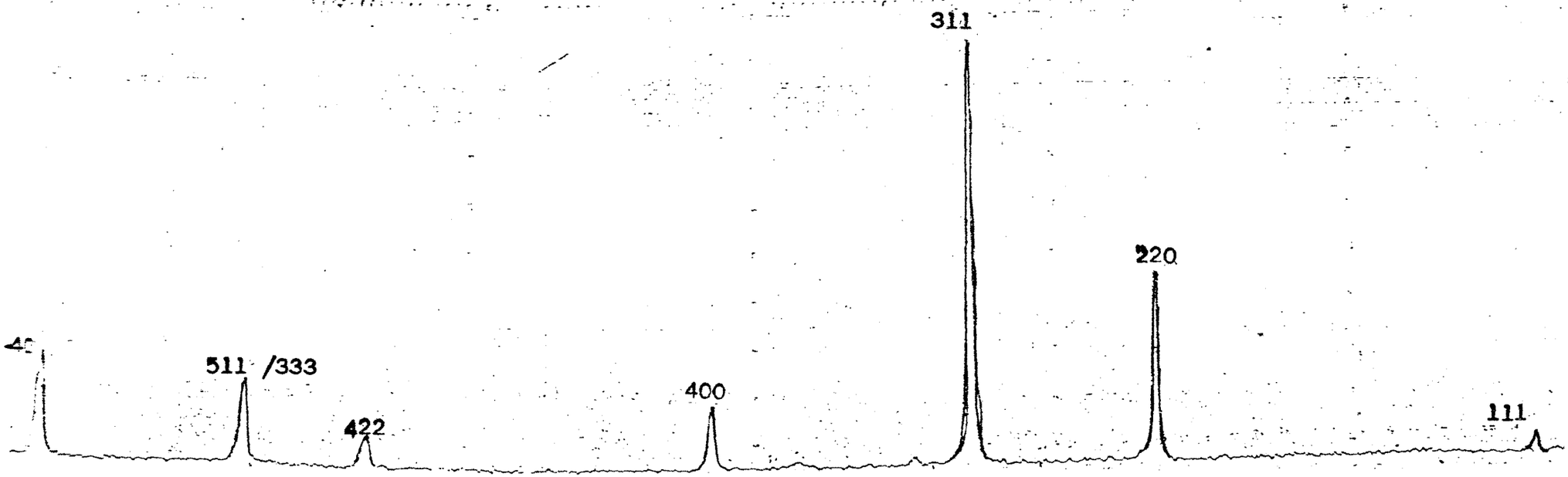

FIG ; 2.9. - $Zn_{0.6}Mg_{0.4}Fe_2O_4$ (L6)

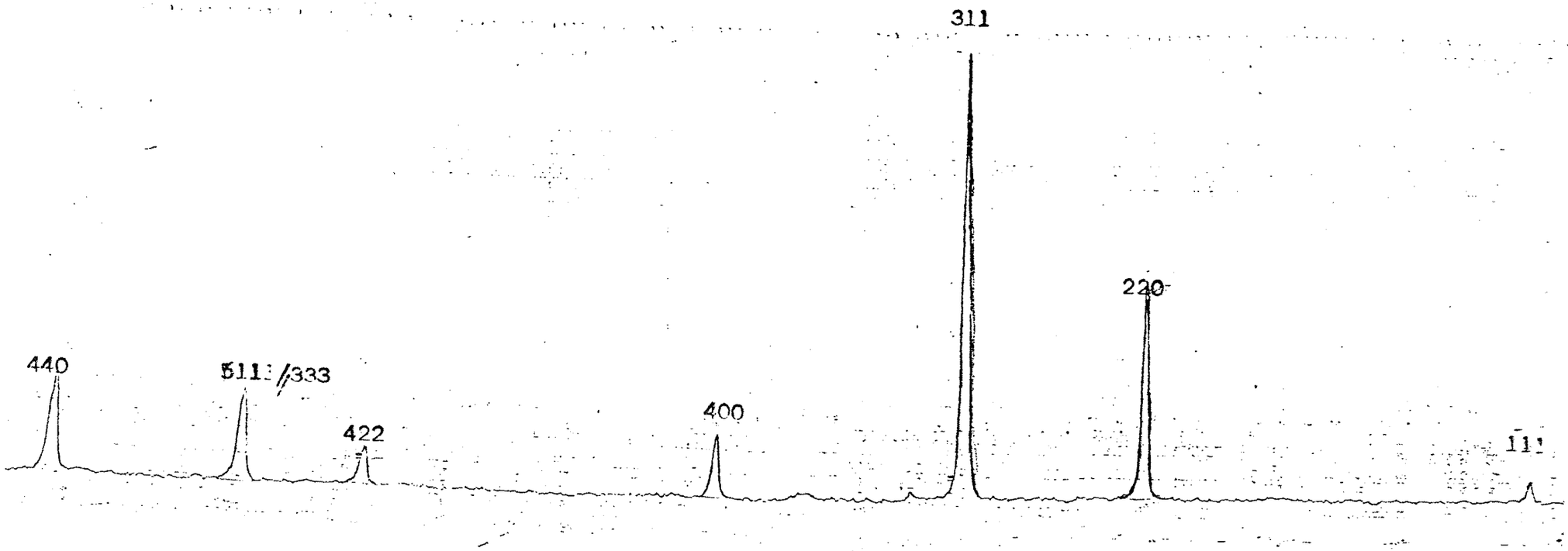

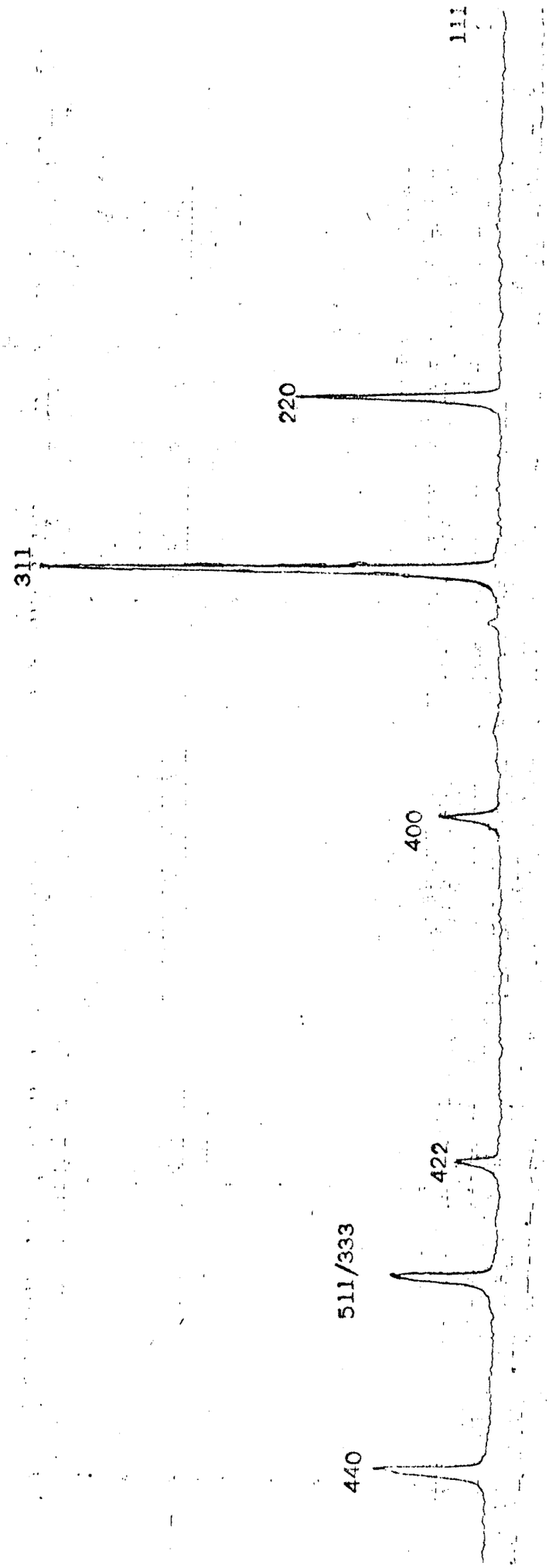

FIG : 2.10- $Zn_{0.8}Mg_{0.2}Fe_2O_4$ (L8)

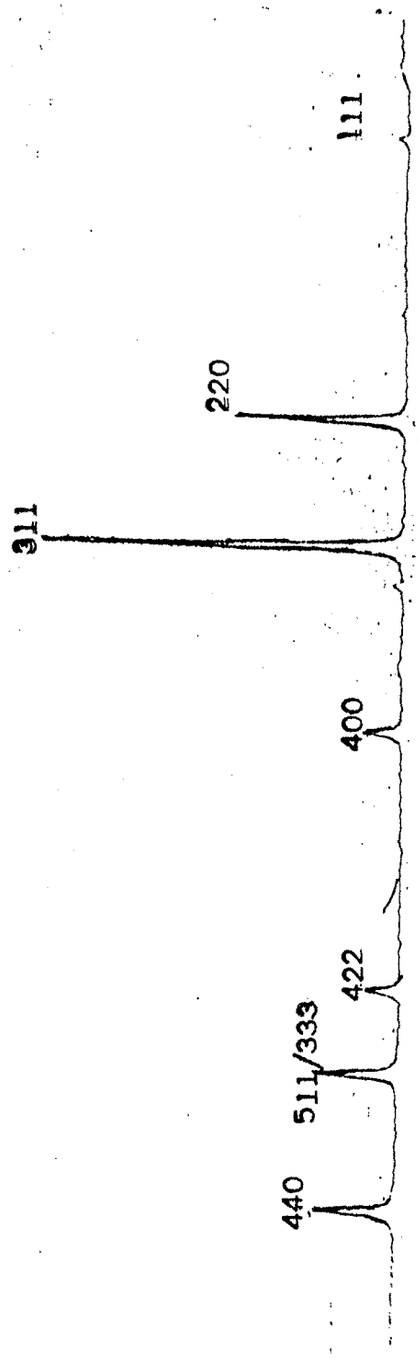

FIG : 2.11 - $Zn\ Fe_2O_4$ (LIC)

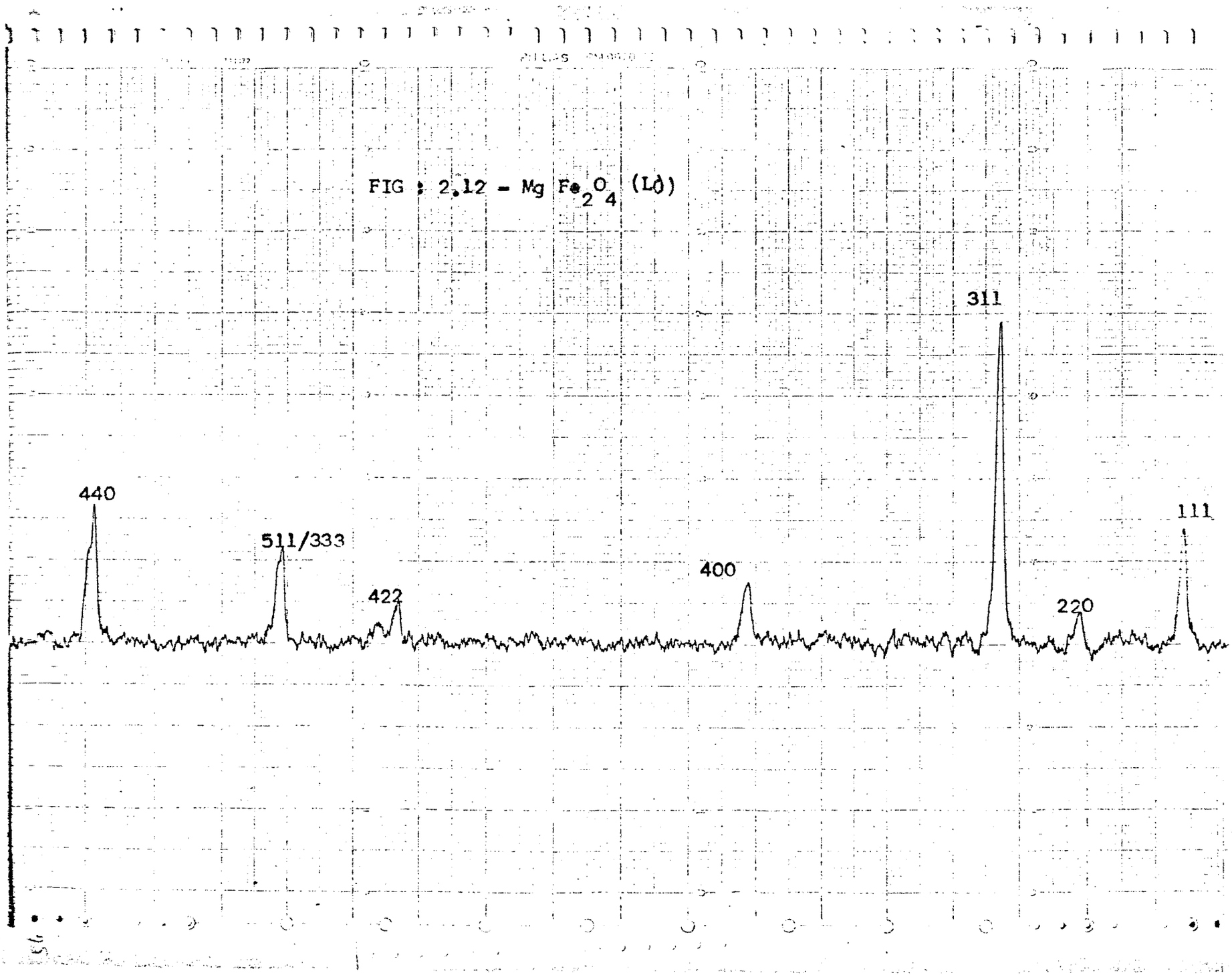

FIG : 2.12 - Mg Fe_2O_4 (LO)

FIG : 2.13- $Zn_{0.2}Mg_{0.8}Fe_2O_4$, Doped (L2)

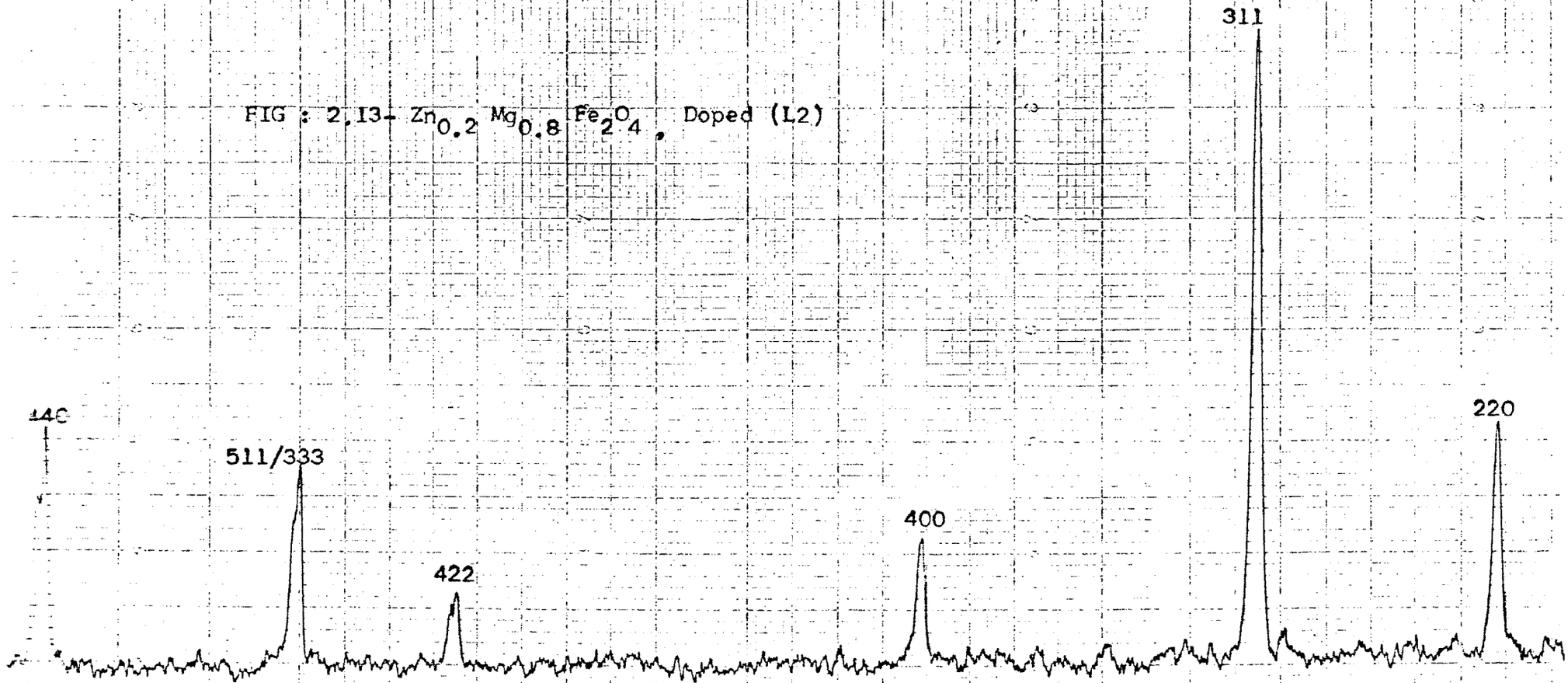

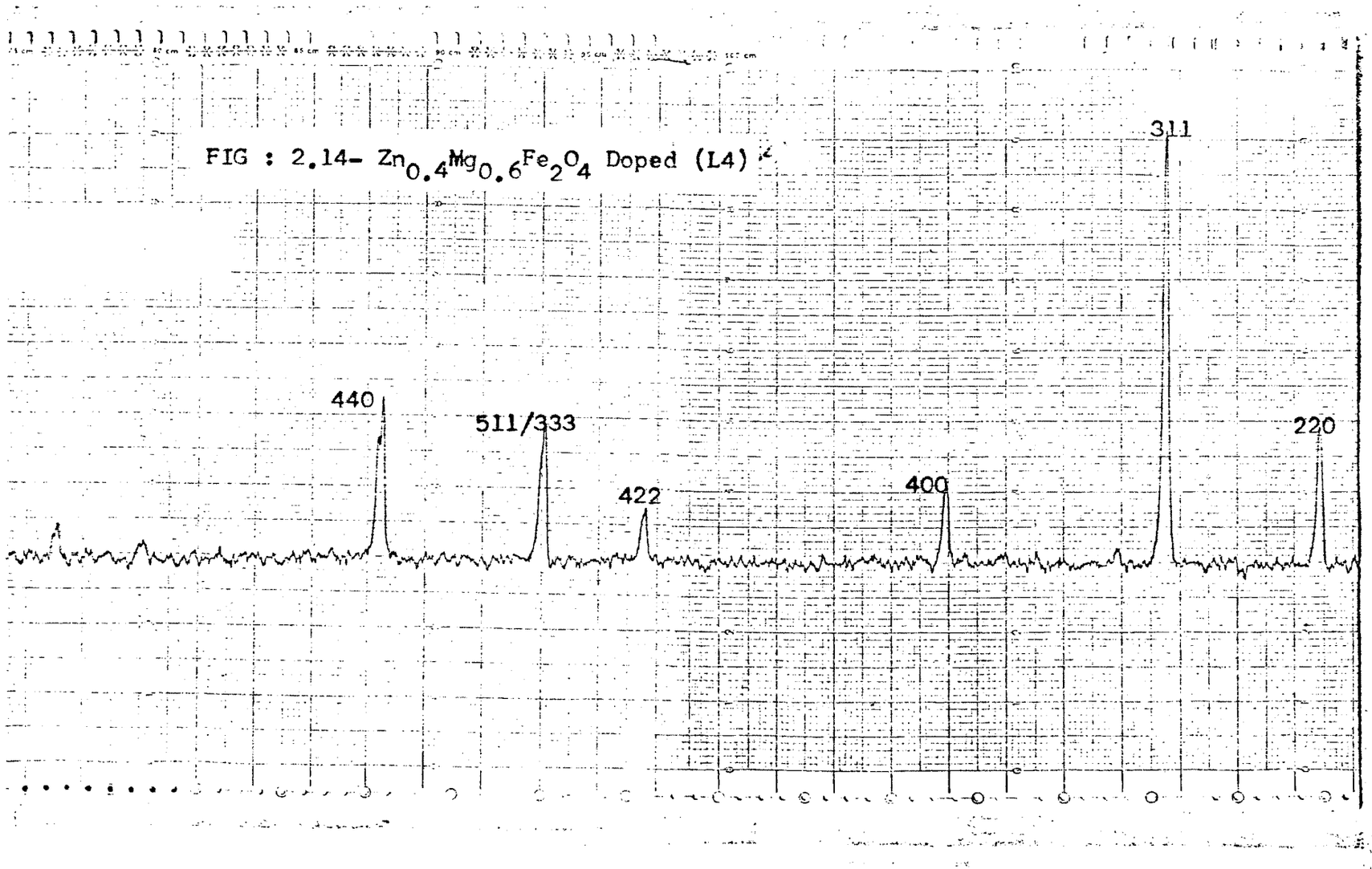

FIG : 2.14- $Zn_{0.4}Mg_{0.6}Fe_2O_4$ Doped (L4)

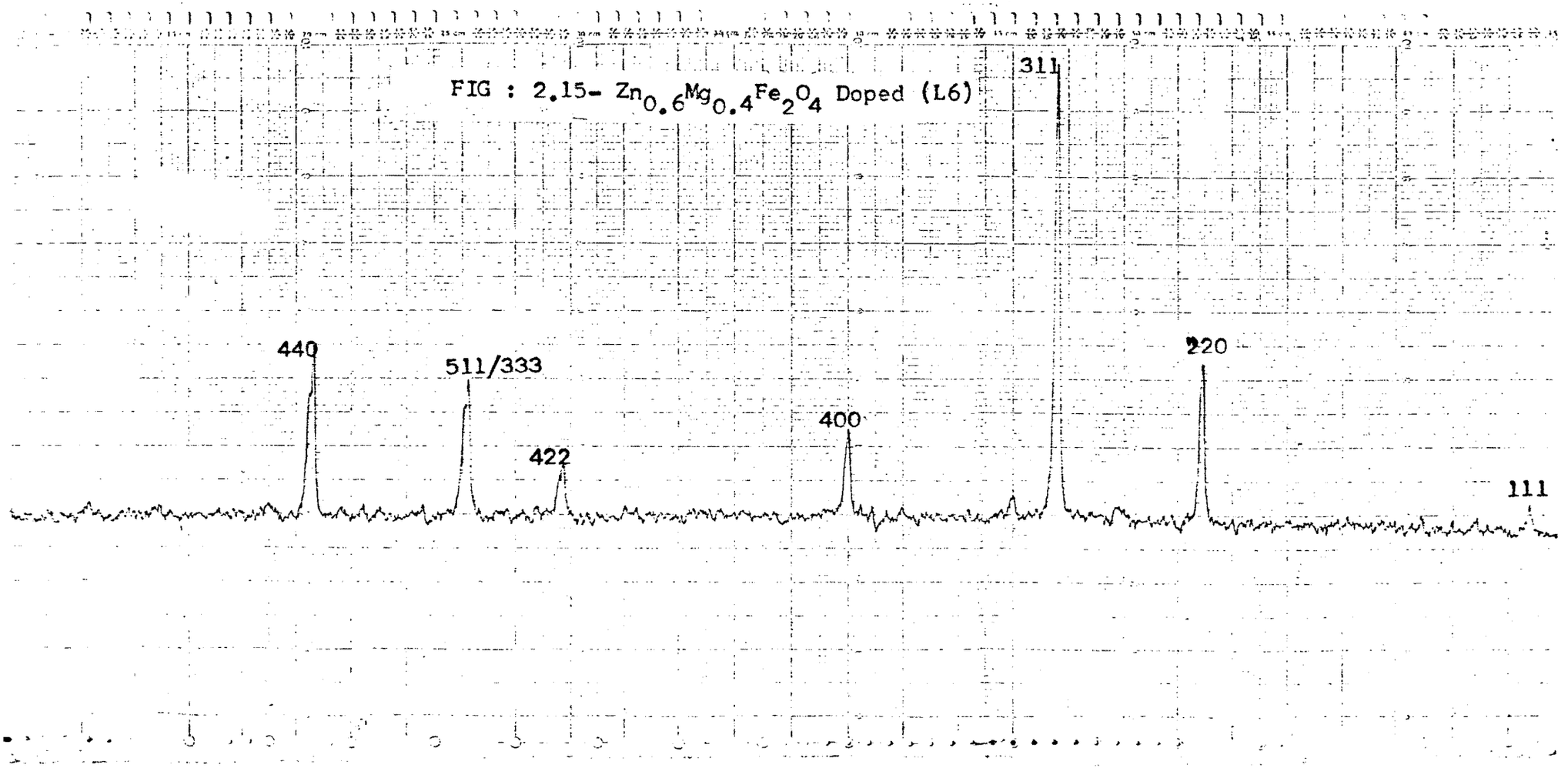

FIG : 2.15- $Zn_{0.6}Mg_{0.4}Fe_2O_4$ Doped (L6)

FIG : 2.16 - $Zn_{0.8}Mg_{0.2}Fe_2O_4$ Doped (18)

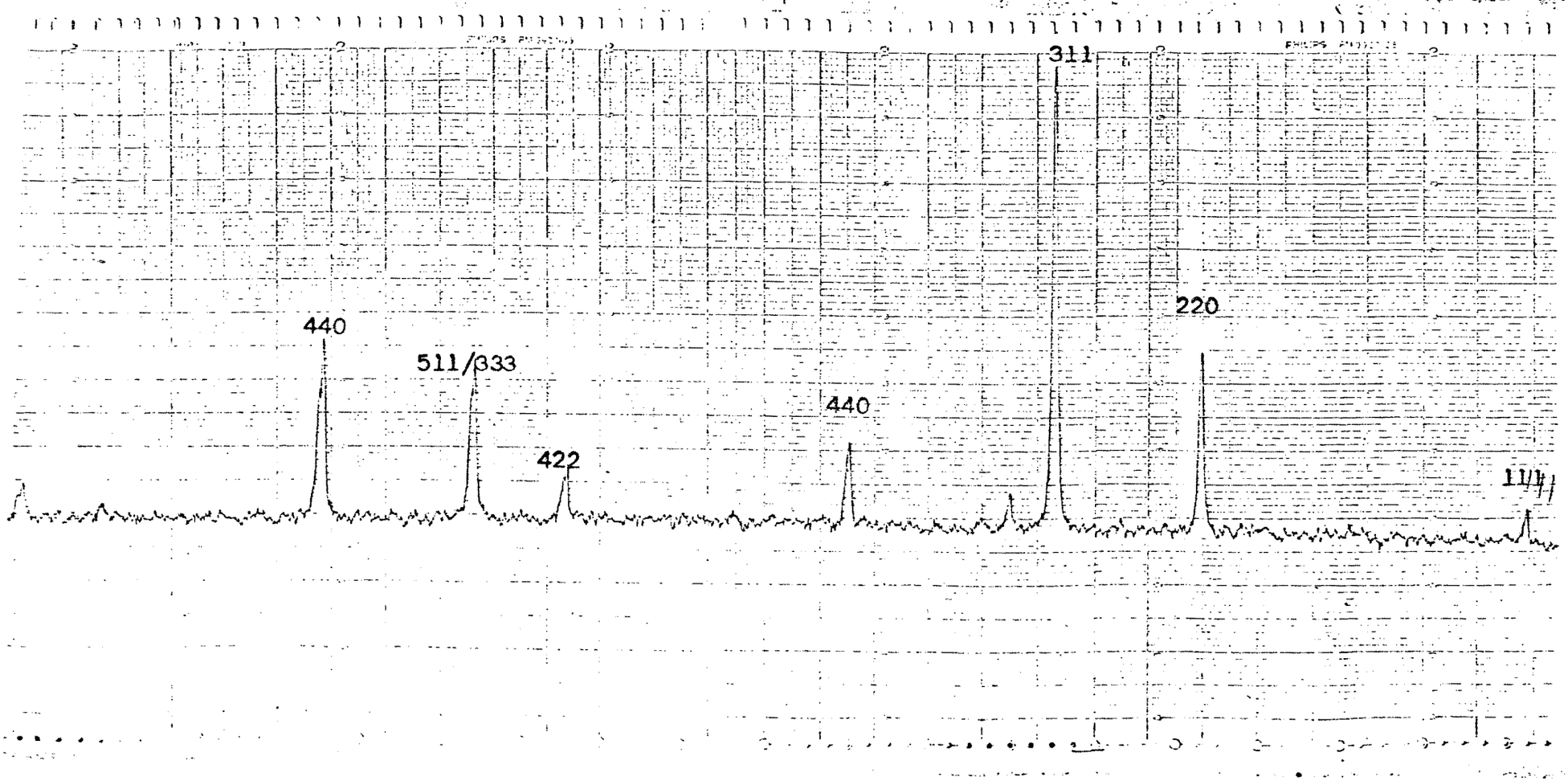

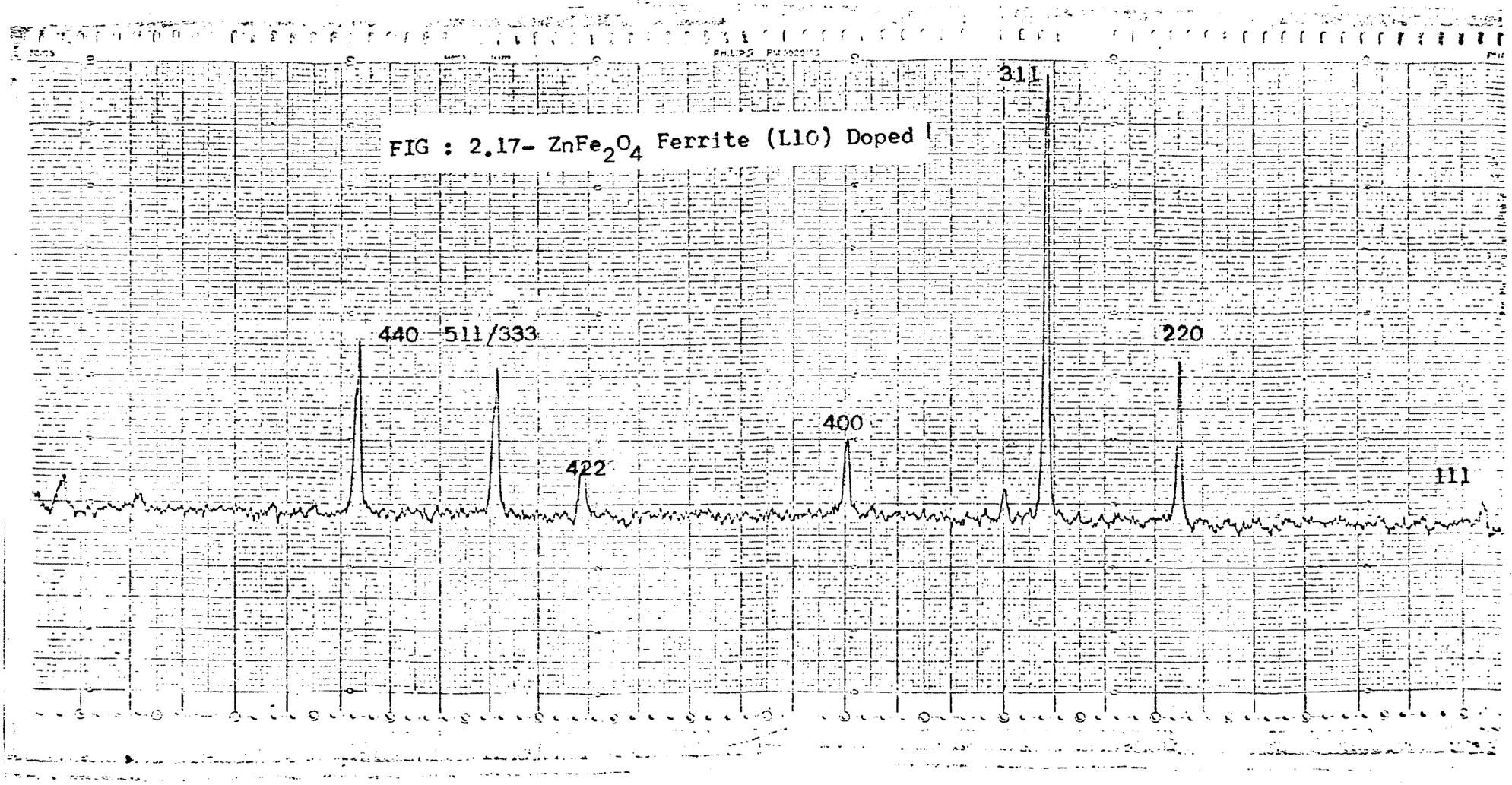

FIG : 2.17- $ZnFe_2O_4$ Ferrite (L10) Doped

Table 2.1 : X-ray diffraction study of $MgFe_2O_4$ ferrite.

Sample - L_0, slow cooled. a = 8.36 A°

2 θ degree	Observed d A°	Calculated d A°	Planes h k l
21.25	4.85	4.87	1 1 1
35	2.98	2.98	2 2 0
41.3	2.54	2.54	2 1 1
43.2	2.43	2.44	2 2 2
50.2	2.11	2.11	4 0 0
63.05	1.72	1.72	4 2 2
67.5	1.62	1.62	5 1 1 3 3 3
74.35	1.49	1.49	4 4 0

Table 2.2 : X-ray diffraction study of $Zn_{0.2}Mg_{0.8}Fe_2O_4$ ferrite.

Sample - L_2, Slow cooled. a = 8.37 A°

2 θ degree	Observed d A°	Calculated d A°	Planes h k l
18.5	5.56	5.56	1 1 1
33.5	3.10	3.10	2 2 0
40.4	2.59	2.59	3 1 1
50.52	2.09	2.09	4 0 0
63.8	1.79	1.79	4 2 2
68.4	1.59	1.59	5 1 1 3 3 3
75.8	1.45	1.45	4 4 0

Table 2.3 : X-ray diffraction study of $Zn_{0.4}Mg_{0.6}Fe_2O_4$ ferrite.

Sample - L_4, slow cooled a = 8.39.

2 θ degree	Observed d A°	Calculated d A°	Planes h k l
18.4	5.59	5.60	1 1 1
33.1	3.10	3.10	2 2 0
39.9	3.07	3.07	3 1 1
50.4	2.10	2.10	4 0 0
63.8	1.69	1.69	4 2 2
69.4	1.57	1.57	5 1 1
76.8	1.44	1.44	4 4 0

Table 2.4 : X-ray diffraction study of $Zn_{0.6}Mg_{0.4}Fe_2O_4$ ferrite.

Sample L_6, slow cooled, a = 8.4 A°

2 θ degree	Observed d A°	Calculated d A°	Planes h k l
21.5	4.79	4.79	1 1 1
35	2.97	2.97	2 2 0
41.3	2.54	2.54	3 1 1
52.5	2.02	2.02	4 0 0
62.8	1.71	1.71	4 2 2
67.4	1.61	1.61	3 3 3 5 1 1
74.4	1.48	1.48	4 4 0

Table 2.5 : X-ray diffraction study of $Zn_{0.8}Mg_{0.2}Fe_2O_4$ ferrite.

Sample L_8, slow cooled a = 8.43 A°

2 θ degree	Observed d A°	Calculated d A°	Planes h k l
19.6	5.13	5.14	1 1 1
34.1	3.05	3.05	2.2 0
40.8	2.56	2.56	3 1 1
50.3	2.10	2.10	4 0 0
63.2	1.70	1.70	4 2 2
67.8	1.60	1.63	3 3 3
			5 1 1
75	1.47	1.47	4 0 0

Table 2.6 : X-ray diffractiion study of $ZnFe_2O_4$ ferrite.

Sample L_{10}, slow cooled a = 8.44 A°

2 θ degree	Observed d A°	Calculated d A°	Planes h k l
21.4	4.81	4.84	1 1 1
35.3	2.95	2.96	2 2 0
41.6	2.52	2.53	3 1 1
50.6	2.09	2.10	4 0 0
63.1	1.71	1.71	4 2 2
67.5	1.61	1.61	5 1 1
			3 3 3
74.4	1.48	1.48	4 4 0

Table 2.7 : X-ray diffraction study of $MgFe_2O_4$ ferrite doped with 0.01 mol. wt. % ZrO_2

Sample L_0, slow cooled. a = 8.36 A°

2 θ degree	Observed d A°	Calculated d A°	Planes h k l
30.2	2.95	2.95	2 2 0
35.6	2.51	2.51	3 1 1
43.2	2.09	2.09	4 0 0
53.6	1.70	1.70	4 2 2
57.2	1.60	1.60	5 1 1
			3 3 3
62.8	1.47	1.47	4 4 0

Table 2.8 : X-ray diffraction study of $Zn_{0.2}Mg_{0.8}Fe_2O_4$ ferrite doped with 0.01 mol. wt.% ZrO_2

Sample L_2, Slow cooled a = 8.37 A°

2 θ degree	Observed d A°	Calculated d A°	Planes h k l
30.2	2.95	2.95	2 2 0
35.4	2.53	2.53	3 1 1
43.1	2.10	2.10	4 0 0
53.5	1.71	1.71	4 2 2
57	1.61	1.54	3 3 3
			5 1 1
62.6	1.48	1.48	4 4 0

Table 2.9 : X-ray diffraction study of $Zn_{0.4}Mg_{0.8}Fe_2O_4$ ferrite doped with 0.01 mol. wt. % ZrO_2

Sample L_4, slow cooled. a = 8.39 A°

2 θ degree	Observed d A°	Calculated d A°	Planes h k l
30.2	2.95	2.95	2 2 0
35.4	2.53	2.53	3 1 1
43	1.71	1.71	4 0 0
53.4	1.72	1.72	4 2 2
56.9	1.61	1.61	3 3 3 5 1 1
62.4	1.48	1.48	4 4 0

Table 2.10 : X-ray diffraction study of $Zn_{0.6}Mg_{0.4}Fe_2O_4$ ferrite doped with 0.01 mol. wt. % ZrO_2.

Sample L_6, slow cooled a = 8.41 A°

2 θ degree	Observed d A°	Calculated d A°	Planes h k l
18.3	4.84	4.84	1 1 1
30	2.97	2.97	2 2 0
35.4	2.53	2.53	3 1 1
43	1.71	1.71	4 0 0
53.2	1.94	1.87	4 2 2
56.8	1.82	1.61	3 3 3 5 1 1
62.4	1.48	1.48	4 4 0

Table 2.11 : X-ray diffractioin study of $Zn_{0.8}Mg_{0.2}Fe_2O_4$ ferrite doped with 0.01 mol. wt. % ZrO_2

Sample - L_8, slow cooled a = 8.43 A°

2 θ degree	Observed d A°	Calculated d A°	Planes h k l
18.2	5.50	5.48	1 1 1
30	2.97	2.97	2 2 0
35.4	2.53	2.53	3 1 1
42.9	2.37	2.10	4 0 0
53.2	1.94	1.72	4 2 2
56.7	1.74	1.62	3 3 3
			5 1 1
62.3	1.66	1.66	4 0 0

Table 2.12 : X-ray diffraction study of $ZnFe_2O_4$ ferrite doped with 0.01 mol. wt.% ZrO_2

Sample L_{10}, slow cooled a = 8.44 A°

2 θ degree	Observed d A°	Calculated d A°	Planes h k l
18.2	5.50	5.48	1 1 1
30	2.95	2.97	2 2 0
35.35	2.56	2.53	3 1 1
42.9	2.37	2.10	4 0 0
53.2	1.94	1.92	4 2 2
56.7	1.79	1.62	3 3 3
			5 1 1
62.2	1.68	1.68	4 0 0

Table 2.13 : The crystallographic data of slow cooled $Zn_xMg_{1-x}Fe_2O_4$ ferrite system (Undoped)

Composition	Sample Notation	Lattice Parameter a A°	X-ray density ρ_x gm/cm³	Physical density gm/cm³ ρ_s	Porosity $\frac{\rho_x-\rho_s}{\rho_x}\times 100$	A - O A°	B - O A°	r_A A°	r_B A°
$MgFe_2O_4$	L_0	8.36	4.55	3.09	31.93	1.8186	2.0698	0.5768	0.7198
$Zn_{0.2}Mg_{0.8}Fe_2O_4$	L_2	8.37	4.71	3.23	31.40	1.8996	2.0405	0.5796	0.7228
$Zn_{0.4}Mg_{0.6}Fe_2O_4$	L_4	8.39	4.88	3.16	35.22	1.9023	2.0434	0.5823	0.7257
$Zn_{0.6}Mg_{0.4}Fe_2O_4$	L_6	8.40	5.03	3.21	36.24	1.9059	2.0790	0.5859	0.7296
$Zn_{0.8}Mg_{0.2}Fe_2O_4$	L_8	8.43	5.15	3.63	29.90	1.9287	2.0282	0.6225	0.7047
$ZnFe_2O_4$	L_{10}	8.44	5.32	3.82	27.77	1.9734	2.0291	0.6534	0.7056

Table 2.14 : The crystallographic data of slow cooled $Zn_xMg_{1-x}Fe_2O_4$ ferrite system doped with 0.01 mol. wt.% ZrO_2.

Composition	Sample Notation	Lattice Parameter a A°	X-ray density ρ_x gm/cm³	Physical density gm/cm³ ρ_s	Porosity $\frac{\rho_x - \rho_s}{\rho_x} \times 100$	A - O A°	B - O A°	r_A A°	r_B A°
$MgFe_2O_4$	L_0	8.36	4.54	3.10	31.69	1.8973	2.0411	0.7203	0.5773
$Zn_{0.2}Mg_{0.8}Fe_2O_4$	L_2	8.37	4.68	3.48	25.70	1.9030	2.0473	0.7265	0.5822
$Zn_{0.4}Mg_{0.6}Fe_2O_4$	L_4	8.39	4.89	3.64	25.30	1.9032	2.0475	0.7267	0.5824
$Zn_{0.6}Mg_{0.4}Fe_2O_4$	L_6	8.41	5.03	3.72	25.91	1.9660	2.010	0.6979	0.6457
$Zn_{0.8}Mg_{0.2}Fe_2O_4$	L_8	8.43	5.17	3.79	26.79	1.9698	2.01422	0.7018	0.6495
$ZnFe_2O_4$	L_{10}	8.44	5.34	3.97	25.88	1.9711	2.01562	0.7032	0.6509

comparative statement 2.13 and 2.14 it can be seen that the lattice parameter 'a' remains almost unaffected by addition of 0.01 mol. wt. % ZrO_2

The crystallographic data of addition of 0.5 mol. wt.% V_2O_5 in Ni-Zn ferrite by Ram Narayan[32] et. al. also shows no variation in the lattice parameter 'a ' From table 2·13 and 2·14 it can be seen that the lattice parameter shows the same trend of variation with increase of zinc content before and after doping In both cases 'a is found to increase with increase of zinc content This is due to the larger ionic radius of Zn^{2+} ion (0.74 Å); when substituted for the divalent metal ion in the lattice, which replaces the smaller Fe^{3+} ion 1. 67 A in the A site[33] The graph of variation of lattice parameter a with zinc content for both before and after doping is given in figure 2.18 and 2.19.

The various parameters such as bond distances A-O, B-O and ionic radii r_A , r_B are calculated for both system before and after doping using the formulae given in section 2.7. The comparative statement of these parameters for the system under investigation, before and after doping is given in tables 2·13 and 2.14 respectively. In calculations of above parameters values of U = 0·381 is used from L_0 to L_4 sample, while u = 0·385 is used from L_6 to L_{10} for both systems. Both systems before and after doping show the same trend of variation with increase of zinc content.

The values of X ray density and percentage porosity in both cases is calculated from the formulae 2.16 and 2.15 respectively. The variation of X-ray density with increase of zinc content shows linear relation in both cases of doped and undoped, however the density of the doped samples is increased. The percentage porosity in both cases is calculated and is given in table 2.13

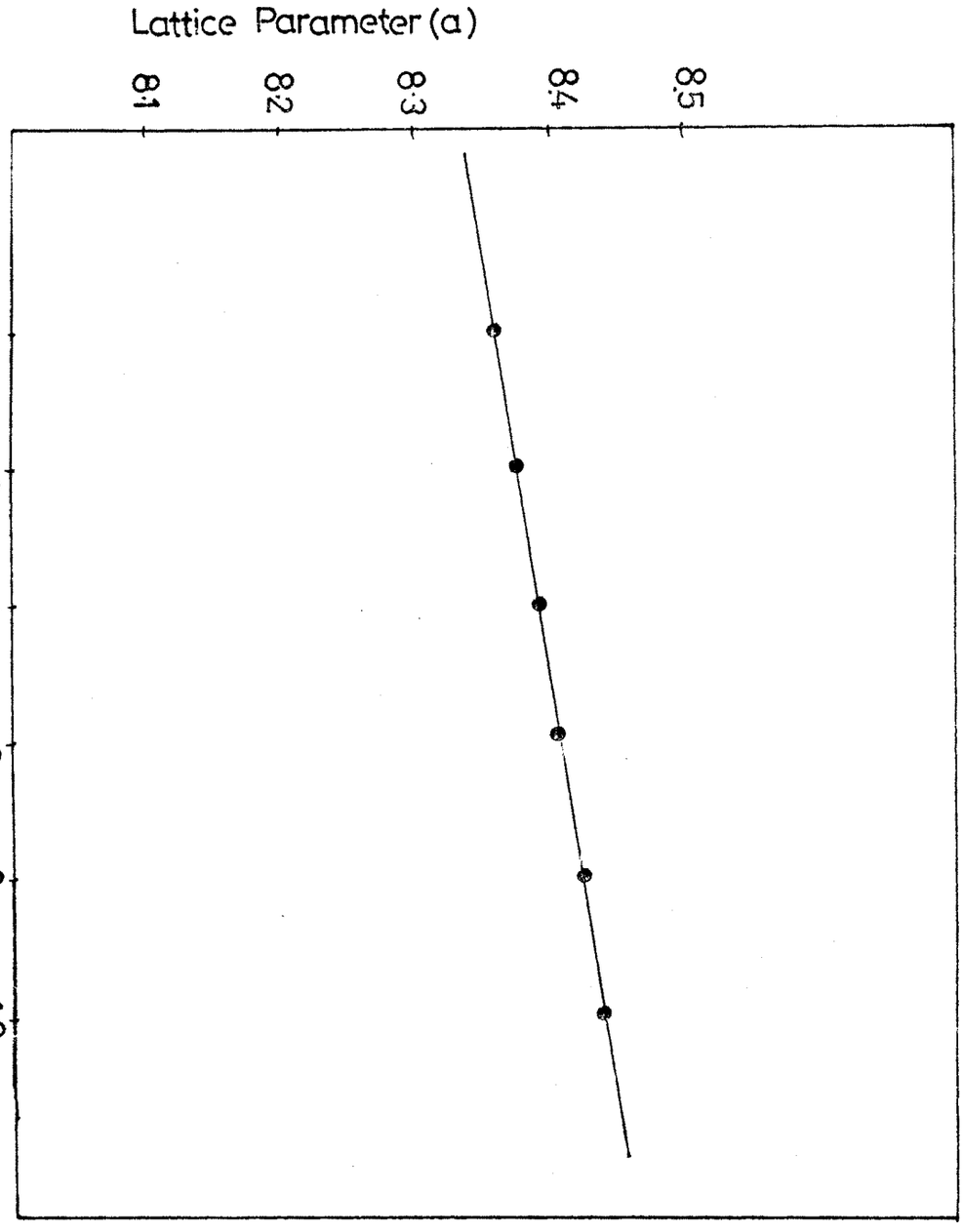

FIG - 2.18 Lattice Parameter Vs Zn Content

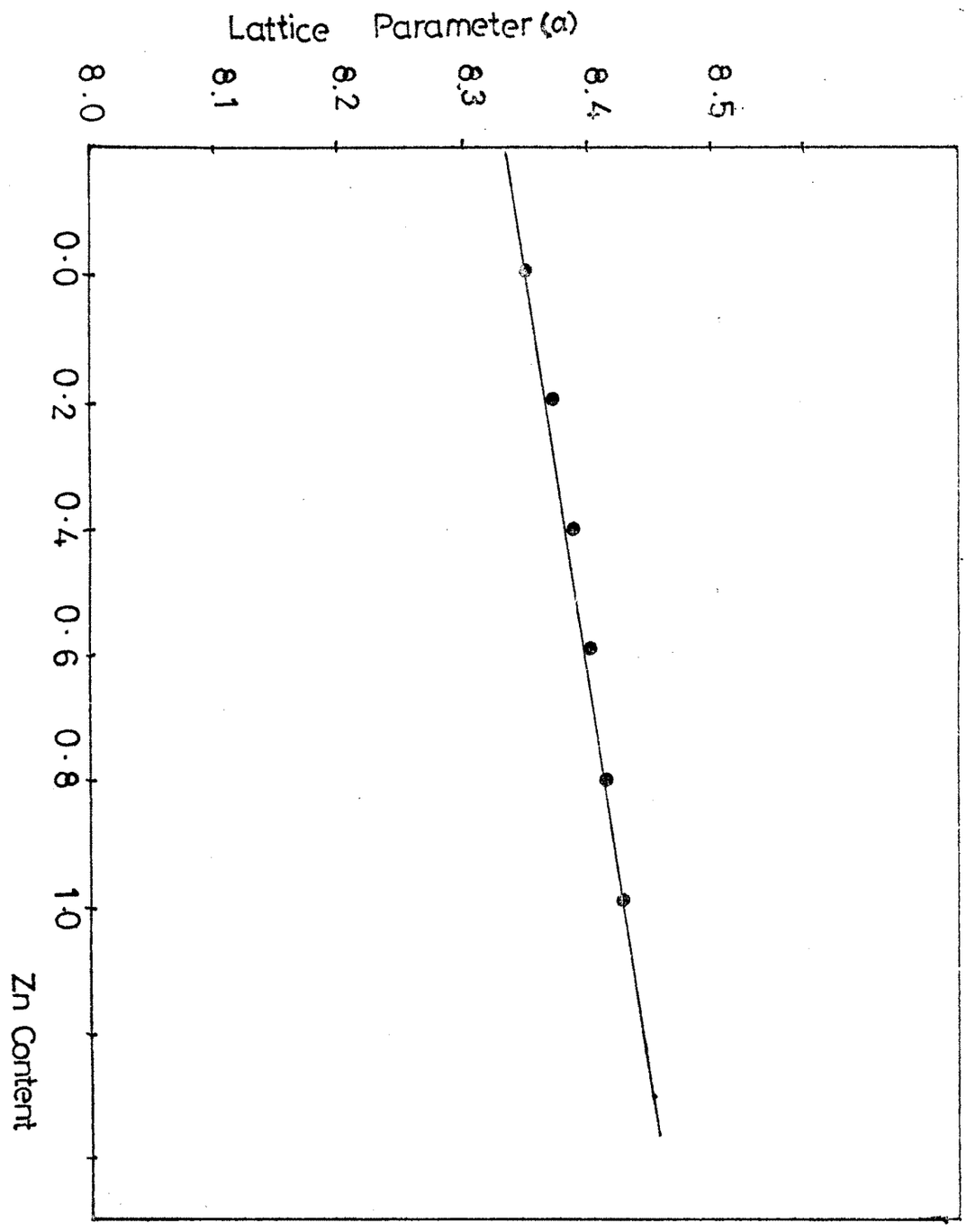

FIG- 2.19 : Lattice Parameter Vs. Zn Content

and 2·14. In doped system the values of percentage porosity are lower than that of undoped system. This can be attributed to the fact that the doped quantity may get dissolved into the lattice of $Zn_xMg_{1-x}Fe_2O_4$ ferrite system. This may be resulted in the densification of the samples and observed reduction in percentage porosity. The doped quantity thus goes to interstitial positions and fills some pores. The similar study of doping of V_2O_5 in Ni-Zn ferrite by Ram Narayan et. al.[34] also have reported the densification effect .

REFERENCES

1) Balckman L.C.F., Trans.Br.Ceram.Soc., 56, 624 (1957).

2) K.J.Standley, "Oxide Magnetic Material", chap.2, p.9. Clearendon Press, Oxford (1972).

3) G.Economas, J.Ame.Cera. Soc., 38, 241 (1955).

4) W.P.Wolf, G.P.Rodrigues, J.Appl. Phys., 29, 105 (1958).

5) Sato I.E.E., Trans. Mag., MAG6, 795 (1970).

6) Swallow D. and Jordon A.K. Proc.Br.Ceram.Soc. 2, 1 (1964).

7) K.J.Standley, "Oxide Magnetic Materials Chap.2, page.No.11, Clearendon Press Oxford (1972).

8) Parkeen, L.S. and Gurry, R.W., J.Am.Chem.Soc., 44, 216 (1945).

9) Smiltens J., J.Chem.Phys. 20, 990 (1952).

10) Paladino A.E., J.Am.Ceram.Soc., 43, 193 (1960).

11) Woodhouse and White, J.Trans.Brit.Ceram.Soc., 54, 33 (1955).

12) C.Zener, See. Smith Trans. A.I.M.E., 175, 15 (1948).

13) Reijnen - P.J.L., Sci.Ceram. 4, 169 (1968).

14) Ram Prasad and Moorthy V.K., Trans. Ind. Ceram. Soc., 29(4), 91 (1970).

15) Oudemans G.J. and Gruintjes G.S., Ceram Bull., 411 (1966).

16) De. Lau. J.G.M., Proc. Br. Ceram. Soc., 10, 275 (1968).

17) Murry P., Livey D.T. and Williams J., "Ceramic Fabrication Process", W.D.Kingery (ed.) Willey, New York, p.147 (1958).

18) Guillaud C., J.Physics Radium, 12, 239 (1951).

19) Goodenough J.B. and Loeb A.L., Physics Rev. 98, 391 (1955).

20) Vaingankar A.S., Patil S.A. and Sahasrabudhe V.S., Trans. Indian Inst. Metals, 34 No.5, 387 (1981).

21) John E. Thompson, "The magnetic Properties of Ferrites", The Himalayan Publishing Group,Ltd., Middlesex, England (1968).

22) Hudson A.S., I Cream M.A., 'Review of microwave ferrites and Garnets', The Marconi Review, 1, 55 (1970).

23) Wyckoff R.W.G., Crystal structures Vol.I and II, Interscience, New York (1951).

24) Gorter E.W. Proc. I. R. E. 1453 (1955).

25) Sinha A.P.B. and Menon P.G. 'Solid state Chemistry' Ed. by C.N.R.Rao, Marcel Dekker, Inc. New York, p. 385 (1974).

26) 'Magnetic properties of material' Ed. by Smit J., Inter University Electronics Series, New York, 13, 22 (1971 ed.)

27) Mikheev V.I. Dokl. Akad. Nauk S.S.S.R., 101, 343 (1955).

28) Bragg W.H. and Bragg W.L. Proc. Roy. Soc., London (A), 88, 428 (1923).

29) B.D. Cullity, "Elements of X-ray diffractions" Addison Wesley Publishing Company, Inc. England (1959).

30) N.S.Satyamurthy, M.G.Natera and S.I. Yousseff, Phys. Rev. 181, 969 (1969).

31) Smit J. and Wijn H.D.J. Ferrites Jon Willey and Sons, New York, 1959, 369 pp.

32) Ram Narayan, R.B.Tripathi, B.K.Das, G.C.Jain, J.Mater. Sci. 18, 1267 (1983).

33) R.G.Kulkarni, Solid State Communication Vol.48, No.8 691-695 (1953).

****